nature chemical biology

ARTICLES

Gene expression signatures and small-molecule compounds link a protein kinase to *Plasmodium falciparum* motility

Nobutaka Kato[1,2], Tomoyo Sakata[2], Ghislain Breton[1], Karine G Le Roch[2], Advait Nagle[2], Carsten Andersen[2], Badry Bursulaya[2], Kerstin Henson[1,2], Jeffrey Johnson[1], Kota Arun Kumar[3], Felix Marr[1], Daniel Mason[2], Case McNamara[2], David Plouffe[2], Vandana Ramachandran[1], Muriel Spooner[2], Tove Tuntland[2], Yingyao Zhou[2], Eric C Peters[2], Arnab Chatterjee[2], Peter G Schultz[1,2], Gary E Ward[4], Nathanael Gray[2], Jeffrey Harper[5] & Elizabeth A Winzeler[1,2]

Calcium-dependent protein kinases play a crucial role in intracellular calcium signaling in plants, some algae and protozoa. In *Plasmodium falciparum*, calcium-dependent protein kinase 1 (PfCDPK1) is expressed during schizogony in the erythrocytic stage as well as in the sporozoite stage. It is coexpressed with genes that encode the parasite motor complex, a cellular component required for parasite invasion of host cells, parasite motility and potentially cytokinesis. A targeted gene-disruption approach demonstrated that *pfcdpk1* seems to be essential for parasite viability. An *in vitro* biochemical screen using recombinant PfCDPK1 against a library of 20,000 compounds resulted in the identification of a series of structurally related 2,6,9-trisubstituted purines. Compound treatment caused sudden developmental arrest at the late schizont stage in *P. falciparum* and a large reduction in intracellular parasites in *Toxoplasma gondii*, which suggests a possible role for PfCDPK1 in regulation of parasite motility during egress and invasion.

Plasmodium spp. are intracellular protozoan parasites in the phylum Apicomplexa, many members of which are human and/or animal pathogens. *P. falciparum* is responsible for the most lethal form of malaria, resulting in an annual mortality of over 1 million people[1]. Other prominent members of the phylum include *Toxoplasma gondii*, one of the most common causes of congenital neurological defects in humans; *Eimeria* spp., poultry and cattle pathogens; *Cryptosporidia*, opportunistic human and animal pathogens; and *Theileria*, a cattle parasite. Much of the pathogenesis associated with these parasitic diseases is due to repeated cycles of host-cell invasion, intracellular replication and host-cell lysis. Therefore, understanding parasitic cell cycle progression is essential for the development of new antimalarial drugs and vaccines.

In the vertebrate host, the parasite undergoes two main phases of development—the hepatic and erythrocytic phases—but it is only the erythrocytic phase of its life cycle that causes severe pathology. During the erythrocytic phase, the parasite goes through a complex but well-synchronized series of stages, which suggests the existence of tightly regulated signaling pathways. It has been known that the presence of calcium in the medium used in the culture of *P. falciparum* is required for parasite invasion of erythrocytes and that chelating calcium in infected erythrocytes results in developmental arrest and impairs parasite invasion in culture[2,3]. This suggests that calcium serves as an intracellular messenger to control synchronization and development in the erythrocytic phase. Calcium is a ubiquitous messenger in eukaryotic intracellular signaling, and calcium binding/sensing proteins play a key role in translating calcium transients generated by external stimuli into cellular responses.

Many of these calcium binding/sensing proteins have EF hands (well-conserved helix-loop-helix calcium binding motifs), and numerous genes having EF-hand motifs have been identified in *Plasmodium* spp. genomes[4]. Calcium-dependent protein kinases (CDPKs), the best characterized EF hand–possessing proteins in Apicomplexa, are most closely related to calmodulin-dependent protein kinases (CaMKs)[5] on the basis of sequence homology. Found only in plants, some algae and apicomplexan protozoa, there are at least five annotated CDPKs in each *Plasmodium* genome[5]. Among these *Plasmodium* CDPKs, *P. berghei* CDPK3 and CDPK4 (PbCDPK3 and PbCDPK4) have been shown to be involved in mosquito stages. PbCDPK4 has been demonstrated to be essential for sexual reproduction in the midgut

[1]Department of Cell Biology, The Scripps Research Institute, 10550 North Torrey Pines Road, ICND202 La Jolla, California 92037, USA. [2]Genomics Institute of the Novartis Research Foundation, 10675 John Jay Hopkins Drive, San Diego, California 92121, USA. [3]Michael Heidelberger Division of Immunology, Department of Pathology, New York University School of Medicine, 550 First Avenue, New York, New York 10016, USA. [4]Department of Microbiology and Molecular Genetics, University of Vermont, 95 Carrigan Drive, Burlington, Vermont 05405, USA. [5]Biochemistry Department, University of Nevada, 1664 North Virginia Street, Reno, Nevada 89557, USA. Correspondence should be addressed to E.A.W. (winzeler@scripps.edu).

Received 31 December 2007; accepted 4 April 2008; published online 4 May 2008; doi:10.1038/nchembio.87

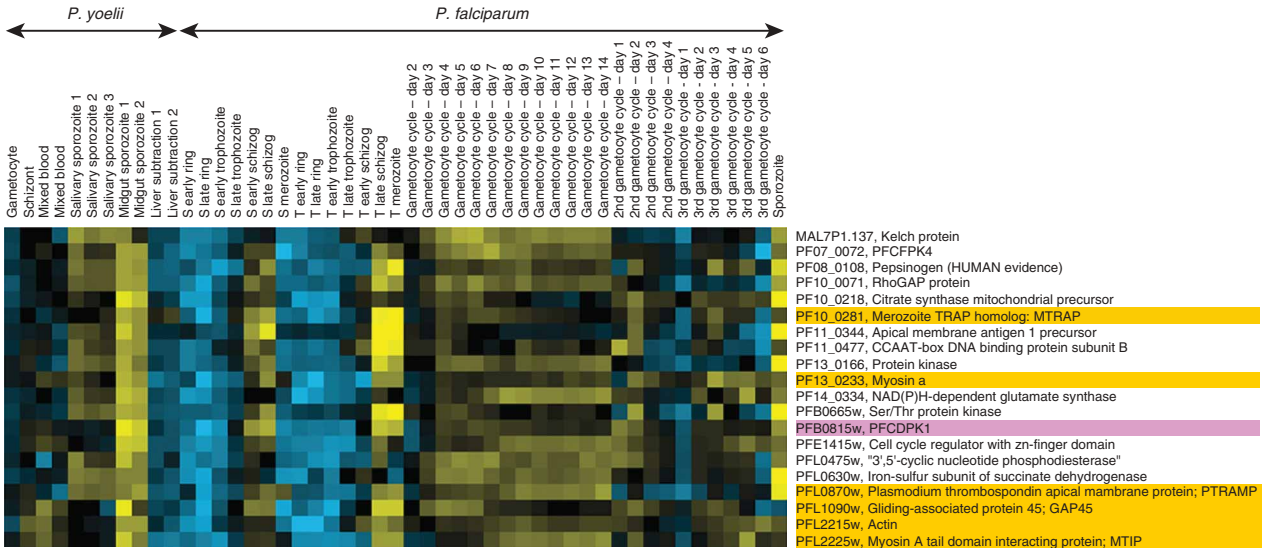

Figure 1 *pfcdpk1* is coexpressed with genes involved in parasite motility. Normalized transcription patterns were derived from expression profiling of different *P. falciparum*[9,12] and *P. yoelii* cultures obtained from different life cycle stages. *P. yoelii* and *P. falciparum* orthologs were mapped to one another and hierarchically coclustered as previously described[12]. The image shows the group of 20 genes from an expression cluster of 50 derived genes (only fully or partially characterized genes are shown) that have been co-cited in a manuscript describing parasite motility[14]. Given that there were 2,317 genes that were clustered, the probability of this enrichment of motility genes occurring by chance is very low ($<10^{-20}$). *pfcdpk1* (PfB0815w) is highlighted in pink, and genes with roles in parasite motility are highlighted in orange. Peptides mapping to the PfCDPK1 protein have been detected by tandem mass spectrometry exclusively in *P. falciparum* merozoites, which supports mRNA expression data. Parasite motility is thought to be a calcium-dependent process, which suggests a possible biological role for the protein.

of the mosquito by translating the calcium signal into a cellular response and regulating cell cycle progression in the male gametocyte[6]. PbCDPK3 regulates ookinete gliding motility and penetration of the layer covering the midgut epithelium[7,8].

On the other hand, transcripts of *P. falciparum* CDPK1 (PfCDPK1) are present during schizogony of blood stages and in the infectious sporozoite stage[9], and the protein is secreted into the parasitophorous vacuole by an acylation-dependent mechanism[10]. It may be myristoylated, and it is abundantly found in detergent-resistant membrane fractions isolated from schizogonic-stage parasites[11]. Here we show, using analysis of gene expression data from several *Plasmodium* species and life cycle data, that *pfcdpk1* clusters with genes associated with parasite motility. In addition, we identify inhibitors of PfCDPK1 activity and show that treatment of the malaria parasites with a representative inhibitor, purfalcamine (**1**), causes developmental arrest at the schizont stage. PfCDPK1 phosphorylates the myosin A tail domain–interacting protein (MTIP), one of the parasite motor complex genes, *in vitro*, which suggests a putative role for PfCDPK1 in regulation of myosin function in the process of parasite motility.

RESULTS

Ontology-based pattern identification analysis

In order to determine a potential physiological function of PfCDPK1, we applied a clustering routine called ontology-based pattern identification[12] to the gene expression data derived from both *P. falciparum* and *P. yoelii*[13]. This algorithm uses published gene ontologies, literature-derived annotations, or other gene lists to optimize hierarchical cluster boundaries and normalization methods and performs permutation testing to determine which gene expression clusters could be expected by chance. When life cycle gene expression data including sporozoite stage, erythrocytic and gametocytogenesis time courses[13] were analyzed, *pfcdpk1* was placed into a cluster of 50 genes having substantial overlap with a set of genes previously described in the literature as having a role in motility and/or invasion[14]. Genes in this cluster show peak expression at the onset of schizogony and are also transcribed in oocyst-stage sporozoites from *P. yoelii* (**Fig. 1**). Unlike many bacteria or viruses that rely on host cell endocytosis for invasion, apicomplexan parasites rely on calcium-dependent adhesion-based motility driven by an actin-myosin motor to actively penetrate host cells after random contact between the two cells[14–16]. Though many of the genes are hypothetical, 6 of the 20 characterized genes in the cluster are motility-associated proteins, including merozoite thrombospondin-related anonymous protein (MTRAP), actin, myosin A, MTIP (which is important for invasion in merozoite-stage parasites and gliding motility in the sporozoite stage[17,18], and egress in *T. gondii*[19]), *Plasmodium* thrombospondin-related apical membrane protein (PTRAMP) and gliding-associated protein 45 (GAP45). Although there is less documentation, it is also possible that some of these motor proteins play a role in cytokinesis and formation of merozoites. Given that there are few known motility-associated proteins, this enrichment is highly significant ($\log_{10} P < -7$). Moreover, most of these proteins are found in the micronemes, an organelle involved in invasion and found only in the sporozoite and merozoite stages. It has been shown for *T. gondii* that an increase in intracellular calcium stimulates microneme discharge[20] and that the contents of micronemes are eventually found in parasitophorous vacuoles. While coexpression does not necessarily indicate a common functional role, the data suggest a possible role for PfCDPK1 in regulation of parasite motility in schizogony.

Disruption of *pfcdpk1*

In order to determine whether or not *pfcdpk1* was likely to be essential for parasite viability and thus a good drug target, we cloned the 5′ and 3′ ends of *pfcdpk1* (PFB0815w) into the pHHT disruption vector

(**Supplementary Fig. 1a** online)[21]. This vector contains both positive and negative selectable markers (thymidine kinase and human dihydrofolate reductase, respectively) and is designed to excise the part of the gene situated between the two regions inserted into the plasmid and replace it with the WR99210 (2) resistance cassette after negative selection for a double recombination event. Parasites were transfected as previously described[21], positive selection with WR99210 was applied for 7 weeks, and then parasites were grown for 3 weeks without drug. Drug treatment resulted in a substantial decrease in parasitemia. The drug pressure was reapplied and parasites were cultured for several more weeks before the negative drug selection with ganciclovir (3) was applied. Genomic DNA was extracted from WR99210-resistant parasites and analyzed on a whole-genome microarray containing ~300,000 25-mer probes to the *P. falciparum* genome. These data showed that *pfcdpk1* was still present and that both lines carried duplications of the upstream and downstream region. In contrast, when the same approach was applied to *pfcdpk4* (PF07_0072), the data showed a complete loss of signal in the central part of the gene, thereby confirming gene replacement. Given the role of the PbCDPK4 in gametocytogenesis[6], these results are not surprising. These data argue that *pfcdpk1* is essential for parasite viability in the erythrocytic stage of the life cycle, whereas the related calcium-dependent protein kinase is not (**Fig. 2**). These findings were the result of two independent transfections and were also confirmed by PCR (**Supplementary Fig. 1b**).

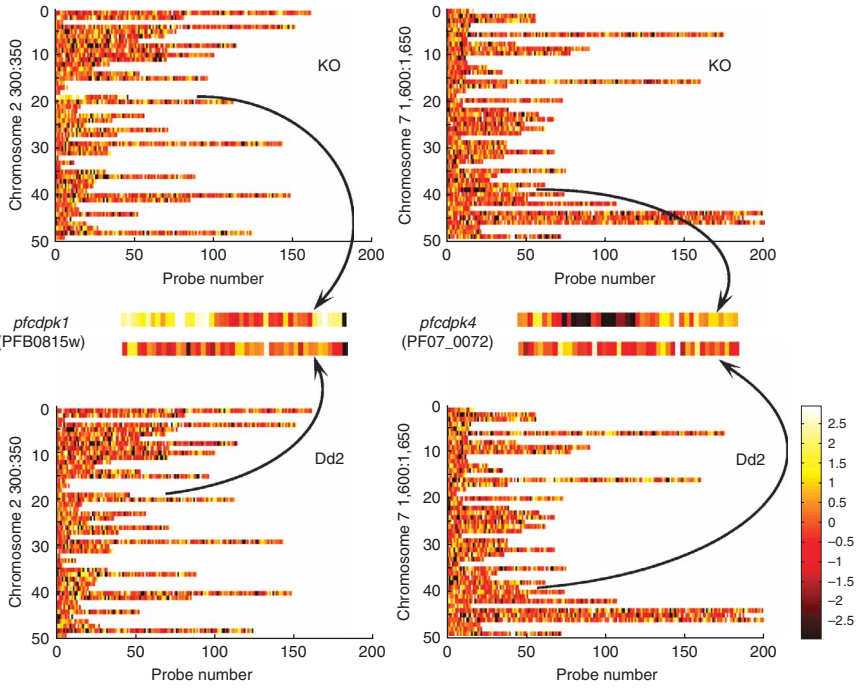

Figure 2 Comparative genome hybridization for knockout strains. *pfcdpk1* (left) and *pfcdpk4* (right) were targeted. Lower panels show the reference strain, Dd2. The image indicates 50 genes (stripes) in the region surrounding the targeted gene, and each square represents the log ratio of the signal at one of the 25-mer probes for a particular gene for the knockout strain to the parent 3D7. Black indicates a loss of signal. These data show a loss of signal for *pfcdkp4* (black) and a gain of signal for the 5′ and 3′ regions of *pfcdpk1*.

In vitro biochemical assay of PfCDPK1

Recombinant PfCDPK1 was expressed as a glutathione S-transferase (GST) fusion protein using the *Escherichia coli* expression system and purified to near homogeneity. Biotinylated casein kinase II peptide (Biotin-RRADDSDDDDD) was identified as a substrate. The reaction conditions were optimized for a scintillation proximity assay as described in Methods. The scintillation proximity assay measures the ability of PfCDPK1 to catalyze the transfer of the γ-phosphate group from [γ-^{33}P]ATP to the biotinylated substrate peptide. The phosphorylated peptides are then captured on streptavidin-coated scintillation beads and activity is quantified in a microtiter plate scintillation counter. When staurosporin (4), a very potent nonselective protein kinase inhibitor, was used at a concentration of 0.5 μM as a positive control and DMSO as a negative control in a 384-well plate format, a Z′ factor value of 0.69 was obtained (**Supplementary Fig. 2** online). The Z′ factor value is a measure of quality of a high-throughput screen to determine which, if any, of the single measurements are significantly different from the negative control, with values above 0.5 indicating a large separation between the values for the positive and negative controls[22].

Compound screening

Approximately 20,000 compounds from a kinase-directed heterocyclic library[23] were screened for their ability to inhibit recombinant PfCDPK1. This assay resulted in the identification of approximately 50 compounds that inhibited kinase activity by greater than 80% at a concentration of 1 μM.

We focused our attention on the most abundant active class, which were derived from the 2,6,9-trisubstituted purine class of kinase inhibitors. As shown in **Table 1**, we determined the half-maximal inhibitory concentration (IC_{50}) values against PfCDPK1 by the scintillation proximity assay and the effector concentration for half maximum response (EC_{50}) values in a parasite proliferation assay for the 13 purines that would provide the most information in regards to structure-activity relationships. This parasite proliferation assay, a modification of published DNA intercalating fluorescent dye–based assays[24,25], was adapted to 384-well plate format and measures the increase in parasite DNA content using the DNA intercalating dye SYBR Green. Compound 1 exhibited strong potency in both the *in vitro* biochemical and parasite proliferation assays, which suggests that this compound is potentially acting against PfCDPK1 *in vivo*. Several other analogs, compounds 7 and 8, exhibited potent enzymatic activity but were inactive in parasite proliferation assays, whereas some analogs displayed low EC_{50} values in the parasite proliferation assay but were inactive against the enzyme. The EC_{50} values of all the compounds may be between four- and five-fold higher in the SYBR Green assay compared to the ^{3}H-hypoxanthine–based assay, which measures incorporation of tritium into DNA[26], as the optimal fluorescent reading conditions required the use of albumax, a lipid-enriched bovine albumin to which small molecules bind. This binding effectively sequesters the drug, thereby reducing the compound concentration and shifting the EC_{50} to a higher value. A shift in the EC_{50} due to albumax was also observed for the reference

Table 1 Structure-activity relationship study of the 2,6,9-trisubstituted purines

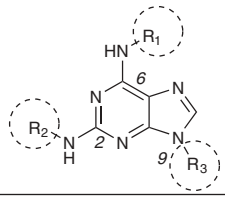

Compound	R_1	R_2	R_3	IC_{50} (nM)	EC_{50} (nM)
1	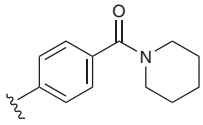	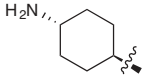	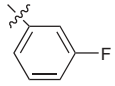	17	230
5			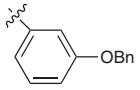	4,040	312
6			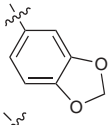	342	400
7			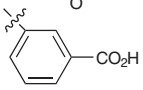	71	>10,000
8			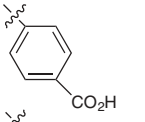	28	>10,000
9			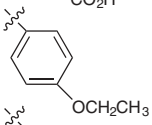	240	535
10			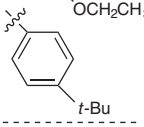	3,490	596
11	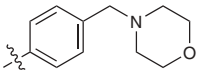			703	174
12	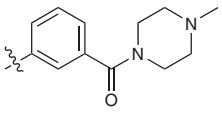	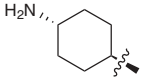		6,870	1,303
13		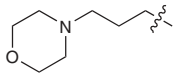		430	2,994
14	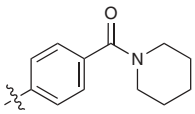	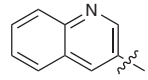		3,846	101
15		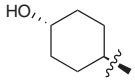	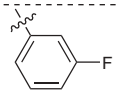	150	>10,000
16		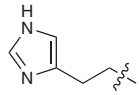	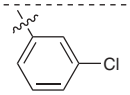	626	352
17	Chloroquine			n.t.	68
18	Artemisinin			n.t.	28
4	Staurosporin			240	n.t.

n.t., not tested.

inhibitors chloroquine (17) and artemisinin (18), which yielded EC_{50} values of less than 10 nM with the 3D7 strain in the ^{3}H-hypoxanthine–based assay under low protein conditions[27,28] but showed an EC_{50} in the same range as the best compound in the parasite proliferation assay (70 nM).

Structure-activity relationship study

Structure-activity relationship studies revealed that the 9-phenyl ring tolerated substitution with small R_3 groups (compounds 1 and 6–9), with most potent enzymatic activity observed for the *m*-fluorine–substituted compound 1 and the carboxy-substituted derivative compounds 7 and 8. However, despite the 200-fold more potent enzymatic activity of compound 1 relative to the *m*-benzylether compound 5, the cellular activity was similar. This suggests that there may be other cellular targets for compound 5 or that compound 1 exhibits reduced cell permeability relative to compound 5. The purine C6-position R_1 group exhibited a strong preference for *p* substitution on the phenyl ring, as evidenced by the complete loss of enzymatic activity and considerable loss of cellular activity for the *m*-substituted compound 12. At the C2-position R_2 group, the 1,4-*trans*-cyclohexane diamine generally resulted in optimal activity. Notably, replacement of the primary amino group at the C2 position with a putatively isosteric hydroxyl to create compound 15 resulted in a complete loss of activity at the cellular level. On the other hand, compound 14 showed cellular activity even with a great loss in enzymatic activity, probably because it contains a quinoline group, which comprises the pharmacophore in a number of antimalaria drugs, such as chloroquine, quinine (19) and mefloquine (20). Because it exhibited the best combined activities on *in vitro* biochemical and parasite proliferation assays, all additional studies were performed on compound 1, which we have named purfalcamine.

Target confirmation by affinity chromatography

In order to examine the selectivity of purfalcamine against PfCDPK1 under more *in vivo*–like conditions, agarose-immobilized purfalcamine was incubated with parasite lysate. After extensive washing, retained proteins were eluted with urea, separated by SDS-PAGE and analyzed by LC/MS/MS. In a separate competition experiment, free purfalcamine (2.5 mM) was added to the parasite lysate and incubated with the agarose-immobilized purfalcamine under identical conditions. LC/MS/MS analysis of

Table 2 List of genes showing significant changes after drug treatment

Peak exp. hrs (cluster)	Representative genes in group	*N*	*M*	*n*	*m*	$\log_{10}P$
Downregulated 48 h						
37 (04)	Etramps, skeleton binding protein, STARP, RESA	1,549	73	93	25	–19.55
38 (15)	MSP1,2,3,5,6,7,8; RAP1,2 CLAG Reticulocyte-binding proteins	1,549	83	78	17	–10.27
Upregulated 48 h						
27 (11)	Proteosome genes	1,549	89	30	5	–2.26
28 (12)	DNA replication genes	1,549	180	81	11	–1.88

Statistically significant enrichment of classes of temporally expressed genes (cluster label 1–15) in genes showing changes after drug treatment. *N*, number of differentially expressed genes previously *k*-means clustered; *M*, number of genes in a given temporal cluster of genes; *n*, number of *N* genes differentially expressed after drug treatment; *m*, number of genes in a cluster showing differential expression. For example, there are 1,549 genes in all 15 cell cycle clusters, among which 73 (4.7%) are in cluster 4. Among the bottom-most 93 genes (in any *k*-means cluster) in the sorted 48-h gene list, 25 (26.9%) actually fall into cluster 4. The *P* value of such an enrichment occurring by chance is 10^{-19}.

trypsin-digested gel lanes from both samples yielded several *P. falciparum* proteins identified by six or more tandem MS spectra in the positive sample but that were not observed in the competition sample, including a hypothetical protein (PF13_01116), a putative FAD-dependent glycerol-3-phosphate dehydrogenase (PFC0275w), a conserved hypothetical protein (PFF0785w) and PfCDPK1. Except for PfCDPK1, no protein kinases or proteins with a recognizable ATP binding site were specifically detected in the positive sample (**Supplementary Fig. 3** and **Supplementary Table 1** online). By contrast, pyruvate kinase (PF10_0363), which is known to be one of the most abundant proteins in the *Plasmodium* intraerythrocytic proteome[29] and which was the only other 'kinase' identified, was detected in both the positive and competition experiments (nine and eight peptides, respectively), and was thus considered to be nonspecific. It is a formal possibility that purfalcamine could be acting against one of the other low-abundance proteins in the list in an unanticipated manner, but this seems unlikely. Dihydroorotate dehydrogenase, for example, is a target of potential interest, although potent biochemical inhibitors of this enzyme are neither similar to purfalcamine nor very active against parasites (for example, 20% inhibition at 10 μM)[30].

Phenotypic analysis of treated parasites

It was our expectation that if purfalcamine is active intracellularly against PfCDPK1 and its kinase activity is required for parasite motility, then inhibitor treatment would result in a reduction in the number of ring-stage parasites that are produced after a merozoite invades a new erythrocyte. To obtain a quantitative assessment of the effect of the compound on the parasite's life cycle, we compared expression profiles of treated and untreated parasites using a full-genome microarray. Heterogeneous, unsynchronized parasites were incubated with 460 nM of purfalcamine for 24 or 48 h. Similar to what we have observed with other drug treatments, several hundred genes showed small (usually less than two-fold) but reproducible changes in transcript levels using a statistical test[31] (**Table 2**, **Supplementary Fig. 4** online). This contrasts with our experience in *Saccharomyces cerevisiae*, in which culture perturbation often results in rapid (after 15 min, not 24 or 48 h) and widespread transcriptional changes, with many genes changing by numerous orders of magnitude[32]. This difference may exist because purfalcamine does not block metabolic pathways, and therefore one would not expect a transcriptional response for a compound that "paralyzes" the parasite. Alternatively, it may exist because apicomplexan parasites have shed the genes involved in transcriptional feedback regulation as they have evolved to become intracellular pathogens. Because we could not find any functional enrichment in the differentially expressed genes using published categories[33], we used previously published classifications that are derived from patterns of gene expression within the parasite life cycle[9]. This analysis showed few changes for 24 h. However, many

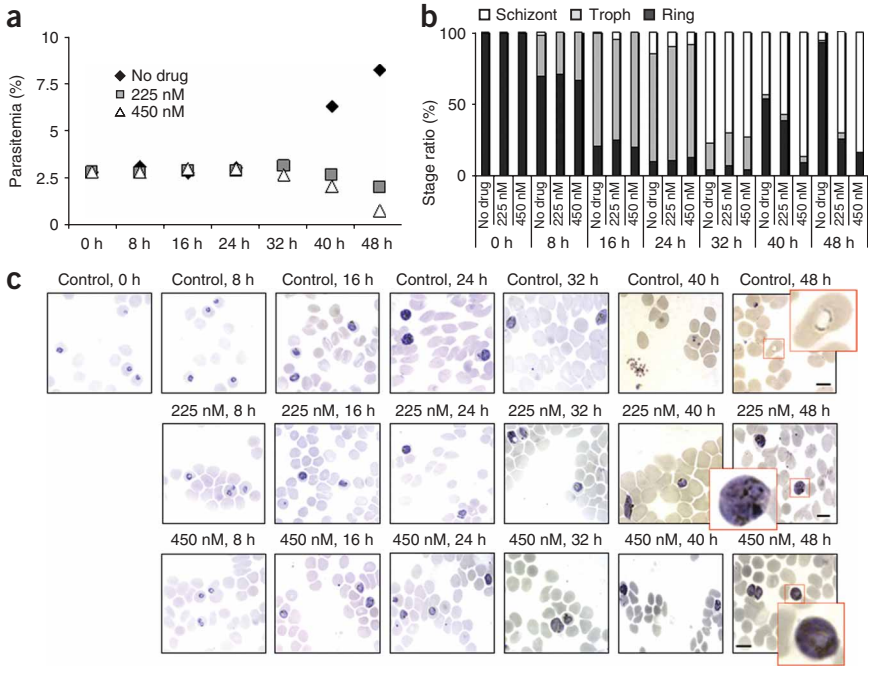

Figure 3 Effect of purfalcamine on parasitemia. Parasites were synchronized twice using the sorbitol method, and purfalcamine was added at the EC_{50} and EC_{90} to the new ring-stage parasites. Parasitemia and morphological change were observed by microscopic examination. (**a**) Effect of different concentration of purfalcamine on parasitemia. (**b**) Effect of purfalcamine on parasite stage compositions. (**c**) Effect of purfalcamine on parasite morphology. Scale bar indicates 10 μm.

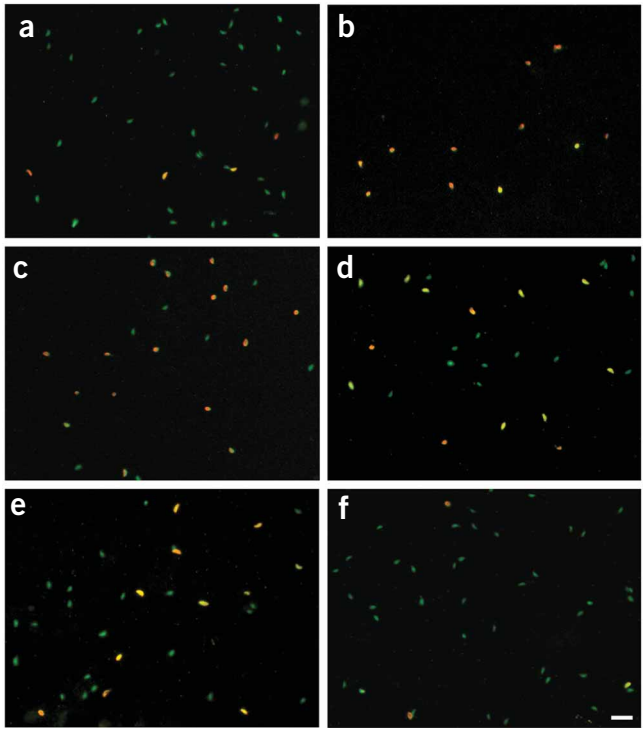

Figure 4 Representative images from a *T. gondii* invasion assay carried out in the presence of varying concentrations of purfalcamine. (**a**–**f**) BS-C-1 cells were incubated with *T. gondii* tachyzoites for 90 min at 37 °C in the presence of 0.8% DMSO (control) (**a**), 100 μM purfalcamine (**b**), 50 μM purfalcamine (**c**), 25 μM purfalcamine (**d**), 12.5 μM purfalcamine (**e**) and 6.25 μM purfalcamine (**f**). External parasites remaining attached to the BS-C-1 cells after sample processing appear both green and red (YFP and Alexa546), and they appear yellow in merged images. Internalized parasites fluoresce green only. Scale bar indicates 20 μm.

genes were downregulated at 48 h of purfalcamine, most of which were found in two previously identified *k*-means clusters whose expression peaked in late schizogony or merozoite stages (37 or 38 h after invasion, clusters 4 and 15). In contrast, many genes showing a late trophozoite expression pattern (27 or 28 h, clusters 11 and 12) showed only slight patterns of induction. Some of the moderately repressed merozoite-stage genes include those encoding merozoite surface proteins (proteins that are important for the formation of the parasitophorous vacuole, such as the early transcribed membrane proteins and ring-specific antigens) and acyl coenzyme A–binding proteins. Although the individual gene changes were relatively unimpressive (for example, merozoite surface protein 3 expression dropped from 510 units to 360 units after treatment, apical membrane protein 1 from 738 to 538 units), the group enrichments were quite significant ($\log_{10}P = -19.55$ for 37 h, –10.27 for 38 h for the downregulated genes). Less significant enrichments were observed among upregulated genes for two groups of trophozoite-expressed genes ($\log_{10}P = -2.26$ and –1.88). These data are consistent with a decrease in the number of merozoite-stage parasites in the culture, as would be expected had the cell cycle been blocked in the late schizont period or in reinvasion. The data also show that expression signatures can provide clues about a compound's mechanism of action.

To confirm these results using established cell biology methods, we synchronized the parasites using a double synchronization with sorbitol (21) treatment and released the ring-stage parasites into medium containing purfalcamine at the EC_{50} and EC_{90} (230 nM and 414 nM, respectively) concentrations. The treated parasites progressed through the cell cycle, increased in size and density and arrested at the late schizogonic stage after DNA replication but potentially before cytokinesis, as segmented schizonts were not observed in the culture. For the first 32 h there was no change in the parasitemia in the two treated cultures. In contrast, after about 40 h, new ring-stage parasites reemerged in the untreated cultures and the parasitemia increased, whereas parasite levels remained stable in the treated culture up to the schizont stage and then began dropping (**Fig. 3**). We also added purfalcamine to synchronized cultures at different time points (12, 24 and 36 h after release of the ring stage) and observed very similar results (**Supplementary Fig. 5** online). These results suggest that purfalcamine has minimal effects, if any, on parasite cell cycle from the ring to early schizogonic stages, but it has its major impact during the late schizogony stage when *pfcdpk1* is transcribed.

In order to better understand the phenotypic effect of the inhibitor, we next tested the activity of purfalcamine in the related apicomplexan parasite *T. gondii*. Extracellular *T. gondii* tachyzoites were treated with various concentrations of purfalcamine and incubated with new host cells. Although purfalcamine was not as active against *T. gondii* as against *P. falciparum*, these data showed that purfalcamine still has potent activity against *T. gondii* and that after treatment extracellular parasites no longer have the ability to invade host cells and remain extracellular (**Fig. 4**, **Supplementary Table 2** online).

In vitro phosphorylation assay

A previous study in which two-hybrid analyses in *P. falciparum* were compared with those of other model organisms indicated that PfCDPK1 might have indirect protein-protein interactions with myosin[34]. Given that myosin light chain protein kinase, one of the CamKs family members, controls smooth muscle contractility in response to intracellular calcium transients, we decided to examine whether PfCDPK1 could phosphorylate PfMTIP, one of the apicomplexan motor complex proteins that is coexpressed with PfCDPK1 (see **Fig. 1**) and a *Plasmodium* ortholog of myosin light chain protein[35]. Mass spectrometric analysis demonstrated that recombinant PfMTIP is recognized as a substrate by recombinant PfCDPK1 under *in vitro* conditions (**Supplementary Fig. 6** online), which further supports our hypothesis that PfCDPK1 might have a role in regulation of myosin function in the process of parasite motility.

Activity against drug-resistant *P. falciparum*

In addition to the 3D7 strain, the potency of purfalcamine was tested on four different *P. falciparum* strains (Dd2, FCB, HB3 and W2), some of which are resistant to common antimalarial drugs such as chloroquine (W2) or pyrimethamine (22) (HB3), and which also carry amplifications in the multidrug resistance protein (Dd2)[36]. Purfalcamine inhibited proliferation of the five strains with nanomolar EC_{50}s (171–259 nM), which indicates effectiveness against drug-resistant parasites (**Supplementary Fig. 7a** online). Given the fact that purfalcamine is acting through a different pathway than chloroquine or pyrimethamine and that the target is highly conserved, this result is not surprising.

Testing pharmacological properties of purfalcamine

Purfalcamine was then tested for toxicity in four mammalian cell lines. Given that the EC_{50} value for *P. falciparum* (3D7) is 230 nM, purfalcamine showed a therapeutic window ranging from 23-fold to 36-fold (EC_{50}s for CHO = 12.33 μM, HEp2 = 7.235 μM, HeLa = 7.029 μM and Huh7 = 5.476 μM). Purfalcamine was also tested in

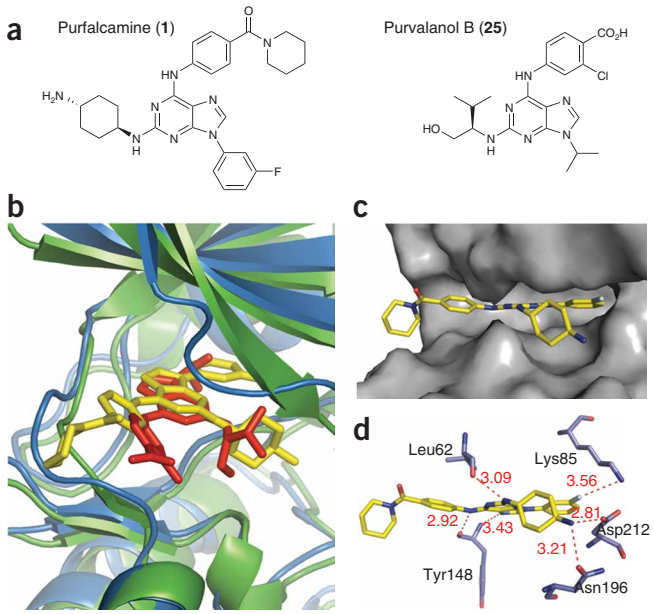

Figure 5 Structure-based ligand docking analysis. Molecular docking studies between a PfCDPK1 homology model and purfalcamine revealed a mode of binding typical of 2,6,9-trisubstituted purines. (**a**) Molecular structures of 2,6,9-trisubstituted purine kinase inhibitors: purvalanol B (**25**) and purfalcamine. (**b**) Comparison of purfalcamine's predicted mode of binding to the cocrystallized complex of *P. falciparum* protein kinase 5 (PfPK5). Shown in cartoon representation, the PfCDPK1 model (blue) was superimposed (r.m.s. deviation 1.48 Å) onto the crystal structure of PfPK5 (light blue). Purfalcamine (yellow) showed similarity in its mode of binding to purvalanol B (red). (**c**) Surface representation of the PfCDPK1 homology model docked with purfalcamine (yellow). (**d**) Analysis of the hydrogen bonding interactions made by purfalcamine (yellow) to residues in the PfCDPK1 ATP binding pocket. The three-letter amino acid code and residue number are labeled next to each side chain. Bonding distances (red) are provided in Å and listed next to each bond (red dashes). PyMOL (http://pymol.sourceforge.net/) was used to generate **b**–**d**.

mice for its pharmacokinetic properties. Purfalcamine exhibited a maximum plasma exposure (C_{max}) of 2.6 ± 0.6 μM with a half-life of 3.1 h. Although the plasma concentrations at 24 h after dosing were close to zero (23 nM), the half-life data suggested that a 10 mg kg^{-1} twice-a-day dosing regimen might be suitable for efficacy studies.

In vivo efficacy studies were carried out on two groups of six mice each. The results demonstrate a delay in the onset of parasitemia in treated mice when compared with control mice (**Supplementary Fig. 7b**), although all the mice eventually needed to be killed. The inability to eliminate parasitemia in blood is likely a combination of the compound being somewhat more selective for the *P. falciparum* enzyme as well as the low exposure and high clearance of the compound in mice. We frequently observe that compounds with lower than 100 nM activity against blood-stage *P. falciparum* parasites are inactive in a four-day Peter's test[37] with rodent parasites. It is likely that the potency would need to be improved to the 10 nM range, or that the pharmacokinetic properties would need to be optimized before the compound could be used as an antimalaria drug.

DISCUSSION

With the exception of artemisinin, drug resistance is prevalent for the most commonly used and approved antimalaria drugs throughout endemic areas. Currently, there are a limited number of antimalarial drugs (and targets), and therefore there is a great demand for new classes of antimalarials. Protein phosphorylation is one of the major post-translational mechanisms used in virtually all intracellular signaling pathways, and protein kinases are now the second most common drug targets after G protein–coupled receptors. About 70–80 enzymes of this family can be found in *P. falciparum* genomic databases[5,38]. Considerable divergence at both the structural and functional levels exists between the vertebrate protein kinases characterized so far and those of their parasites, which lends support to the idea that specific inhibition of parasite enzymes can be achieved[5]. Given that there is a high probability that many of these enzymes are essential to parasite survival, protein kinases are attractive potential drug targets. Furthermore, in the last decade there has been an intense effort in the pharmaceutical sector to develop small-molecule kinase inhibitors that has resulted in a host of diverse chemotypes that can potentially be used as starting points to develop specific *Plasmodium*-targeting drugs.

We have demonstrated that treatment with a PfCDPK1 inhibitor does not affect the erythrocytic development of *P. falciparum* from ring to early schizogony phase, but it does cause the sudden arrest of developmental progression in late schizogony, resulting in a reduction in the number of ring-stage parasites in culture. These findings, along with the results obtained by the ontology-based pattern identification analysis, strongly suggest that PfCDPK1 is involved in regulating parasite motor-dependent processes that occur in the late schizont stage. These may include cytokinesis, egress and invasion, all of which are closely linked in malaria parasites. The molecular mechanisms powering motility appear to be similar in zoites of Apicomplexa[14]. Motility and invasion require release of adhesive proteins from secretory organelles at the apical end of the parasites, including the micronemes, dense granules and rhoptries[20]. Most of the knowledge about apicomplexan motility is derived from studies on the tachyzoites of *T. gondii*[16,39] and *Plasmodium* sporozoites, and these studies reveal a crucial role of calcium transient as a second messenger[40]. Microneme secretion, motility and invasion are not influenced by the levels of extracellular or host cell calcium but do require the release of calcium from intracellular stores. For example, artificially increasing cytoplasmic calcium levels by calcium ionophores is sufficient to induce microneme release in *T. gondii* tachyzoites and *P. falciparum* sporozoites; it is also sufficient to impair parasite motility[20,41]. Even though it is an *in vitro* study and still requires *in vivo* validation, our finding that recombinant PfCDPK1 can phosphorylate recombinant PfMTIP suggests that PfCDPK1 plays a role in regulating parasite motility in response to calcium transitions. Furthermore, KT5926 (**23**), a staurosporin derivative that inhibits many protein kinases including TgCDPK2, has been identified as prominently blocking tachyzoite motility[42]. In humans, CaMKs phosphorylate myosin V tails, resulting in the activation of organelle transport, and it is possible that there is a similar interaction between PfCDPK1 and myosin A[17,18,43] that potentially inhibits microneme secretion.

Though it has been known that PfCDPK1 can also phosphorylate the Raf kinase inhibitor protein *in vitro*[44], the next step would be to identify the *in vivo* substrates of PfCDPK1 and map its signaling pathways. The two-hybrid interaction observed between PfCDPK1 and the cysteine protease SERA8 (PFB0325c) may provide a clue[45]. There is precedence for a phosphorylation event regulating a proteolytic activity. For example, the kinase AKT phosphorylates a serine residue on caspase-9, thus regulating its activity during apotosis[46]. Indeed, a number of proteases, including the protease encoded by *pfsub1* (PFE0370c), are coexpressed with *pfcdpk1*. Before egress, PfSUB1 is secreted into the parasitophorous vacuole and processes SERAs, which in turn likely act on membrane components of the

parasitophorous vacuole and perhaps the erythrocyte to initiate host cell rupture[47,48]. It is noteworthy that the phenotypic effects of compound treatment (prevention of mature merozoites from egress and invasion) by the PfSUB1 inhibitor MRT12113 (**24**)[48] are very similar to the effects of purfalcamine.

Although our results are consistent with inhibition of PfCDPK1 being responsible for the cellular activity of purfalcamine, we cannot rule out the possibility that additional intracellular targets contribute to the cellular activity because structurally related analogs (for example, compound **5**) that are much less active on PfCDPK1 maintain cellular activity. Furthermore, even though it showed strong activity at the level of *in vitro* biochemical and parasite proliferation assays, purfalcamine failed to clear the parasite and only delayed the increase in parasitemia. We believe that this is due to pharmacokinetics properties (low exposure and high clearance) of purfalcamine, and the properties need to be improved without compromising the potency for it to be considered as a lead compound.

Continued optimization of purfalcamine derivatives using structure-based drug design would provide a rational approach and would be a powerful tool to expedite the discovery of derivatives that exhibit even greater specificity and selectivity toward PfCDPK1. In lieu of a cocrystal structure, a computational model of PfCDPK1 docked to purfalcamine was generated (**Fig. 5**). The model shows excellent correlation with the structure-activity relationship analysis, predicts purfalcamine to bind in a mode similar to that of other 2,6,9-trisubstituted purines (**Fig. 5b,c**) and indicates that favorable hydrogen bond contacts are formed with PfCDPK1 residues Lys85, Asn196 and Asp212 (**Fig. 5d**). Of particular interest for optimization is the possible exploitation of inherently variable residues located along the fringe of the PfCDPK1 ATP binding pocket. Nonconserved residues Arg60, Glu149 and Lys202 all reside within bonding distance of the R_1 group and could be targeted as salt bridging partners. In addition, increased selectivity and specificity may be possible by virtue of the moderately sized gatekeeper residue, Thr145, located near the back of the ATP binding pocket. The model shows a substantial gap of space near Thr145 that may accommodate a second, small substituent (for example, methyl or hydroxyl) in either the *para* or remaining *ortho* position in the R_3 group. The model also predicts purfalcamine will have a substantially decreased affinity to other PfCDPKs, despite the fact that these kinases have the highest structural homology to PfCDPK1 in the *P. falciparum* genome (**Supplementary Fig. 8** online). This hypothesis was confirmed with affinity chromatography followed by LC/MS/MS analysis using immobilized purfalcamine, in which PfCDPK1 was the only detected protein kinase. It was further confirmed with *in vitro* biochemical data using recombinant PfCDPK5, which showed a 200-fold increase of the IC_{50} from PfCDPK1 (17 nM) to PfCDPK5 (>3.5 μM). PfCDPK5 exhibits the highest homology to PfCDPK1 among the PfCDPKs, and its transcript is coexpressed with *pfcdpk1*. The combined pharmacological and functional genomics approaches described here suggest that PfCDPK1 is a promising target for a new class of antimalaria drugs.

The need to discover and develop new and inexpensive antimalarial drugs is enormous. Furthermore, because antimalarial drugs will likely be used by people with fewer resources to pay for medicines, keeping synthetic cost down will be important. The trisubstituted purines are synthesized in five or six chemical reaction steps and can be inexpensively manufactured, which makes this compound class attractive as lead compounds for a new class of antimalarial drugs. Moreover, given that these small molecules can be engineered for specificity against many of the 70 or so protein kinases in the *Plasmodium* genome, they hold much promise as chemical tools that can be used to study biological processes with greater precision than can be achieved with conditional mutants.

METHODS

Cultivation of *P. falciparum*. *P. falciparum* (3D7 strain) was cultured in human O^+ erythrocytes as previously described[9]. For synchronizing the parasites, cultures were treated with 5% D-sorbitol[49]. Cells were washed twice in complete RPMI medium following the sorbitol treatment and returned to standard incubation for 48 h to recover from the treatment.

Disruption of *pfcdpk1* and *pfcdpk4*. See **Supplementary Methods** online.

Expression and purification of recombinant PfCDPK1. See **Supplementary Methods**.

Kinase assay using scintillation proximity assay with recombinant PfCDPK1. Kinase activity of the PfCDPK1 was assayed in 20 mM Tris HCl, pH 7.5, $MgCl_2$ 10 mM, EGTA 1 mM, $CaCl_2$ 1.1 mM, 1 μM ATP and 0.1 ng μl^{-1} biotinylated casein. A series of 2,6,9-trisubstituted purines from a 20,000 compound kinase-directed heterocyclic library[23] was screened in 384-well plates. With the exception of the ATP concentration, the kinase assays were performed in the same way for the high-throughput screening (1 μM) and the final IC_{50} measurement (10 μM). Serial dilution of each recombinant enzyme preparation was initially performed for each batch to determine the proper volume. Enzyme and buffer without calcium were mixed and aliquoted (5 μl) in 384-well plates using microplate liquid dispenser. Inhibitors (50 nl of 3 mM) were added using an in-house liquid nanodispenser with a 384-well pintool. ATP and [γ-^{33}P]ATP (0.1 μCi per reaction) were mixed with buffer containing 1.5× calcium and added to the reaction using the microplate liquid dispenser. Kinase reaction was proceeded for 1 h at 24 °C and terminated using 10 μl of a solution containing streptavidin-labeled PVT SPA beads (50 μg per reaction; GE Healthcare), 50 mM ATP, 5 mM EDTA and 0.1% Triton X-100. The SPA beads were spun down in each well by centrifuging for 3 min at 2,000*g*. Incorporated radioactivity was measured using a scintillation counter. Each 384-well compound plate contained staurosporin and purvalanol B as positive controls and DMSO as a negative control, and each compound was screened at least three times. The activities of the selected compounds from the primary screening were reexamined using an independent kinase assay (Kinase-Glo luminescent kinase assay, Promega).

SYBR Green–based parasite proliferation assay. 3D7 *P. falciparum* strain was grown in complete culture medium (RPMI with L-glutamine and without phenol red, 4.3% human serum, 2.08 mg ml^{-1} albumax, 0.013 mg ml^{-1} hypoxantine, 1.17 mg ml^{-1} glucose, 0.18% $NaHCO_3$, 0.031 M HEPES, 2.60 mM NaOH and 0.043 mg ml^{-1} gentamicine) until the parasitemia reached 3% to 8% with O^+ human erythrocytic cells. 20 μl of screening medium (RPMI, 4.16 mg ml^{-1} albumax, 0.013 mg ml^{-1} hypoxantine, 1.73 mg ml^{-1} glucose, 0.18% $NaHCO_3$, 0.031 M HEPES, 2.60 mM NaOH and 0.043 mg ml^{-1} gentamicine) was dispensed into 384-well plates. 50 nl of serially diluted compounds were transferred into the assay plates along with 50 nl of DMSO for the baseline and background control plates. 3D7-infected erythrocytic cell suspension (30 μl) was dispensed into the assay and baseline plates in order to obtain a 2.5% hematocrit and 0.3% parasitemia. 30 μl of noninfected erythrocytic cells were dispensed into the background plate at the same final hematocrit. Plates were incubated for 72 h in a low-oxygen environment (93% N_2, 4% CO_2, 3% O_2). Staining solution (10 μl of 10× SYBR Green solution in RPMI medium) was dispensed into the plates, and the plates were read with the Acquest microplate reader at 520 nm.

Compound library and general synthetic methods. See **Supplementary Methods**.

Target confirmation by affinity chromatography and mass spectrometry. See **Supplementary Methods**.

Expression analysis of drug-treated samples and microscopic analysis. See **Supplementary Methods**.

***T. gondii* invasion assay.** *T. gondii* invasion of BS-C-1 cells was assayed semiquantitatively, as previously described[50]. Briefly, medium containing

various concentrations of purfalcamine or 0.8% (v/v) DMSO (control) was added to confluent BS-C-1 monolayers in 384-well plates, followed immediately by the addition of parasites expressing yellow fluorescent protein. Plates were incubated for 15 min at 23 °C, then for 60–90 min at 37 °C. At the end of the incubation, extracellular parasites were labeled using anti-*T. gondii* monoclonal antibody 11-132 (Argene) followed by Alexa546-conjugated goat anti-mouse IgG. The cells were then washed and fixed, and the extent of invasion in each well was estimated relative to the DMSO control, as described in the legend of **Supplementary Table 2**. Each sample was run in duplicate and scored blind. Images were collected on a Nikon TE300 inverted microscope equipped with epifluorescence illumination using a 100× PlanApo objective (numerical aperture 1.4). Digital images were captured using a SpotRT monochrome camera (Diagnostic Instruments Inc.).

***In vitro* phosphorylation of PfMTIP by PfCDPK1.** See **Supplementary Methods**.

Toxicity and pharmacokinetic studies. HeLa, HEp2, Huh7 and CHO cells were seeded at 250 cells per 8 µl medium (DMEM with 5% fetal bovine serum (HyClone)) per well in a 1,536-well plate. Purfalcamine was transferred the next day and cells were cultured for 72 h to match the incubation length during the parasite proliferation assay. Cellular toxicity was assessed using Cell Titer Glo (Promega).

Purfalcamine was tested in mice for its pharmacokinetic properties. Five- to six-week-old male Balb/c mice (22–25 g) were obtained from Jackson Laboratory. Purfalcamine was dissolved in a 4 mg ml^{-1} solution formulation of 50% captisol (0.6 g l^{-1}), 0.5% HCl and 49.5% sodium phosphate buffer at pH 7.4. The compound was administered as a single dose orally via gavage at 20 mg kg^{-1}. 50 µl blood samples were drawn via retro orbital sinus at five sampling times within 24 h after dosing. Plasma concentrations of these compounds were quantified using a LC/MS/MS assay. Pharmacokinetic parameters were calculated by noncompartmental regression analysis using Winnonlin 4.0 (Pharsight). Animal studies described in this report were performed according to the US Animal Welfare Act and the Guide for the Care and Use of Laboratory Animals, and they were approved by the Institutional Animal Care and Use Committee at the Genomics Institute of the Novartis Research Foundation. All experiments were conducted in a US Department of Agriculture–certified vivarium.

Efficacy studies. See **Supplementary Methods**.

Homology modeling and virtual ligand screening. See **Supplementary Methods**.

Note: Supplementary information and chemical compound information is available on the Nature Chemical Biology website.

ACKNOWLEDGMENTS

We thank V. Nussenzweig (New York University) for providing oocyst and sporozoite stages of *P. yoelii* and A. Godfrey-Certner for her assistance with the *T. gondii* invasion assays. This work was supported by a grant to E.A.W. from the Ellison Foundation, the Keck Foundation and the US National Institutes of Health (AI059472-02), a grant to G.E.W. from the US National Institutes of Health (AI054961), and grants to the Genomics Institute of the Novartis Research Foundation from the Wellcome Trust and the Medicines for Malaria Venture.

Published online at http://www.nature.com/naturechemicalbiology
Reprints and permissions information is available online at http://npg.nature.com/reprintsandpermissions

1. Snow, R.W., Guerra, C.A., Noor, A.M., Myint, H.Y. & Hay, S.I. The global distribution of clinical episodes of *Plasmodium falciparum* malaria. *Nature* **434**, 214–217 (2005).
2. Garcia, C.R. Calcium homeostasis and signaling in the blood-stage malaria parasite. *Parasitol. Today* **15**, 488–491 (1999).
3. Gazarini, M.L., Thomas, A.P., Pozzan, T. & Garcia, C.R. Calcium signaling in a low calcium environment: how the intracellular malaria parasite solves the problem. *J. Cell Biol.* **161**, 103–110 (2003).
4. Nagamune, K. & Sibley, L.D. Comparative genomic and phylogenetic analyses of calcium ATPases and calcium-regulated proteins in the apicomplexa. *Mol. Biol. Evol.* **23**, 1613–1627 (2006).
5. Ward, P., Equinet, L., Packer, J. & Doerig, C. Protein kinases of the human malaria parasite *Plasmodium falciparum*: the kinome of a divergent eukaryote. *BMC Genomics* **5**, 79 (2004).
6. Billker, O. *et al.* Calcium and a calcium-dependent protein kinase regulate gamete formation and mosquito transmission in a malaria parasite. *Cell* **117**, 503–514 (2004).
7. Ishino, T., Orito, Y., Chinzei, Y. & Yuda, M. A calcium-dependent protein kinase regulates *Plasmodium* ookinete access to the midgut epithelial cell. *Mol. Microbiol.* **59**, 1175–1184 (2006).
8. Siden-Kiamos, I. *et al. Plasmodium berghei* calcium-dependent protein kinase 3 is required for ookinete gliding motility and mosquito midgut invasion. *Mol. Microbiol.* **60**, 1355–1363 (2006).
9. Le Roch, K.G. *et al.* Discovery of gene function by expression profiling of the malaria parasite life cycle. *Science* **301**, 1503–1508 (2003).
10. Moskes, C. *et al.* Export of *Plasmodium falciparum* calcium-dependent protein kinase 1 to the parasitophorous vacuole is dependent on three N-terminal membrane anchor motifs. *Mol. Microbiol.* **54**, 676–691 (2004).
11. Sanders, P.R. *et al.* Distinct protein classes including novel merozoite surface antigens in Raft-like membranes of *Plasmodium falciparum*. *J. Biol. Chem.* **280**, 40169–40176 (2005).
12. Young, J.A. *et al.* The *Plasmodium falciparum* sexual development transcriptome: a microarray analysis using ontology-based pattern identification. *Mol. Biochem. Parasitol.* **143**, 67–79 (2005).
13. Zhou, Y. *et al.* Evidence-based annotation of the malaria parasite's genome using comparative expression profiling. *PLoS ONE* **3**, e1570 (2008).
14. Baum, J. *et al.* A conserved molecular motor drives cell invasion and gliding motility across malaria life cycle stages and other apicomplexan parasites. *J. Biol. Chem.* **281**, 5197–5208 (2006).
15. Heintzelman, M.B. Cellular and molecular mechanics of gliding locomotion in eukaryotes. *Int. Rev. Cytol.* **251**, 79–129 (2006).
16. Lovett, J.L. & Sibley, L.D. Intracellular calcium stores in *Toxoplasma gondii* govern invasion of host cells. *J. Cell Sci.* **116**, 3009–3016 (2003).
17. Bergman, L.W. *et al.* Myosin A tail domain interacting protein (MTIP) localizes to the inner membrane complex of *Plasmodium* sporozoites. *J. Cell Sci.* **116**, 39–49 (2003).
18. Green, J.L. *et al.* The MTIP-myosin A complex in blood stage malaria parasites. *J. Mol. Biol.* **355**, 933–941 (2006).
19. Meissner, M., Schluter, D. & Soldati, D. Role of *Toxoplasma gondii* myosin A in powering parasite gliding and host cell invasion. *Science* **298**, 837–840 (2002).
20. Carruthers, V.B. & Sibley, L.D. Mobilization of intracellular calcium stimulates microneme discharge in *Toxoplasma gondii*. *Mol. Microbiol.* **31**, 421–428 (1999).
21. Duraisingh, M.T., Triglia, T. & Cowman, A.F. Negative selection of *Plasmodium falciparum* reveals targeted gene deletion by double crossover recombination. *Int. J. Parasitol.* **32**, 81–89 (2002).
22. Zhang, J.H., Chung, T.D. & Oldenburg, K.R. A simple statistical parameter for use in evaluation and validation of high throughput screening assays. *J. Biomol. Screen.* **4**, 67–73 (1999).
23. Ding, S., Gray, N.S., Wu, X., Ding, Q. & Schultz, P.G. A combinatorial scaffold approach toward kinase-directed heterocycle libraries. *J. Am. Chem. Soc.* **124**, 1594–1596 (2002).
24. Bennett, T.N. *et al.* Novel, rapid, and inexpensive cell-based quantification of antimalarial drug efficacy. *Antimicrob. Agents Chemother.* **48**, 1807–1810 (2004).
25. Smilkstein, M., Sriwilaijaroen, N., Kelly, J.X., Wilairat, P. & Riscoe, M. Simple and inexpensive fluorescence-based technique for high-throughput antimalarial drug screening. *Antimicrob. Agents Chemother.* **48**, 1803–1806 (2004).
26. Chulay, J.D., Haynes, J.D. & Diggs, C.L. *Plasmodium falciparum*: assessment of *in vitro* growth by [3H]hypoxanthine incorporation. *Exp. Parasitol.* **55**, 138–146 (1983).
27. Duraisingh, M.T. *et al.* Linkage disequilibrium between two chromosomally distinct loci associated with increased resistance to chloroquine in *Plasmodium falciparum*. *Parasitology* **121**, 1–7 (2000).
28. Fotie, J. *et al.* Lupeol long-chain fatty acid esters with antimalarial activity from *Holarrhena floribunda*. *J. Nat. Prod.* **69**, 62–67 (2006).
29. Florens, L. *et al.* A proteomic view of the *Plasmodium falciparum* life cycle. *Nature* **419**, 520–526 (2002).
30. Baldwin, J. *et al.* High-throughput screening for potent and selective inhibitors of *Plasmodium falciparum* dihydroorotate dehydrogenase. *J. Biol. Chem.* **280**, 21847–21853 (2005).
31. Barrera, L., Benner, C., Tao, Y.C., Winzeler, E. & Zhou, Y. Leveraging two-way probe-level block design for identifying differential gene expression with high-density oligonucleotide arrays. *BMC Bioinformatics* **5**, 42 (2004).
32. Oshiro, G. *et al.* Parallel identification of new genes in *Saccharomyces cerevisiae*. *Genome Res.* **12**, 1210–1220 (2002).
33. Ashburner, M. *et al.* Gene ontology: tool for the unification of biology. The Gene Ontology Consortium. *Nat. Genet.* **25**, 25–29 (2000).
34. Suthram, S., Sittler, T. & Ideker, T. The *Plasmodium* protein network diverges from those of other eukaryotes. *Nature* **438**, 108–112 (2005).
35. Bosch, J. *et al.* The closed MTIP-myosin A-tail complex from the malaria parasite invasion machinery. *J. Mol. Biol.* **372**, 77–88 (2007).
36. Kidgell, C. *et al.* A systematic map of genetic variation in *Plasmodium falciparum*. *PLoS Pathog.* **2**, e57 (2006).

37. Peters, W. & Robinson, B.L. in *Handbook of Animal Models of Infection* (eds. Zak, O. & Sande, M.) 757–773 (Academic, London, 1999).
38. Srinivasan, A.N. & Krupa, A. A genomic perspective of protein kinases in *Plasmodium falciparum*. *Proteins* **58**, 180–189 (2005).
39. Wetzel, D.M., Chen, L.A., Ruiz, F.A., Moreno, S.N. & Sibley, L.D. Calcium-mediated protein secretion potentiates motility in *Toxoplasma gondii*. *J. Cell Sci.* **117**, 5739–5748 (2004).
40. Keeley, A. & Soldati, D. The glideosome: a molecular machine powering motility and host-cell invasion by *Apicomplexa*. *Trends Cell Biol.* **14**, 528–532 (2004).
41. Gantt, S. *et al.* Antibodies against thrombospondin-related anonymous protein do not inhibit *Plasmodium* sporozoite infectivity in vivo. *Infect. Immun.* **68**, 3667–3673 (2000).
42. Kieschnick, H., Wakefield, T., Narducci, C.A. & Beckers, C. *Toxoplasma gondii* attachment to host cells is regulated by a calmodulin-like domain protein kinase. *J. Biol. Chem.* **276**, 12369–12377 (2001).
43. Karcher, R.L. *et al.* Cell cycle regulation of myosin-V by calcium/calmodulin-dependent protein kinase II. *Science* **293**, 1317–1320 (2001).
44. Kugelstadt, D., Winter, D., Pluckhahn, K., Lehmann, W.D. & Kappes, B. Raf kinase inhibitor protein affects activity of *Plasmodium falciparum* calcium-dependent protein kinase 1. *Mol. Biochem. Parasitol.* **151**, 111–117 (2007).
45. LaCount, D.J. *et al.* A protein interaction network of the malaria parasite *Plasmodium falciparum*. *Nature* **438**, 103–107 (2005).
46. Cardone, M.H. *et al.* Regulation of cell death protease caspase-9 by phosphorylation. *Science* **282**, 1318–1321 (1998).
47. Arastu-Kapur, S. *et al.* Identification of proteases that regulate erythrocyte rupture by the malaria parasite *Plasmodium falciparum*. *Nat. Chem. Biol.* **4**, 203–213 (2008).
48. Yeoh, S. *et al.* Subcellular discharge of a serine protease mediates release of invasive malaria parasites from host erythrocytes. *Cell* **131**, 1072–1083 (2007).
49. Lambros, C. & Vanderberg, J.P. Synchronization of *Plasmodium falciparum* erythrocytic stages in culture. *J. Parasitol.* **65**, 418–420 (1979).
50. Carey, K.L., Westwood, N.J., Mitchison, T.J. & Ward, G.E. A small-molecule approach to studying invasive mechanisms of *Toxoplasma gondii*. *Proc. Natl. Acad. Sci. USA* **101**, 7433–7438 (2004).